Available online at www.sciencedirect.com

ScienceDirect

Advances in Space Research 72 (2023) 565–576

ADVANCES IN SPACE RESEARCH (a COSPAR publication)

www.elsevier.com/locate/asr

Production of a set of lunar regolith simulants based on Apollo and Chinese samples

Y. Cengiz Toklu [a], Nurcan Çalış Açıkbaş [b], Gökhan Açıkbaş [b], Ali Erdem Çerçevik [c,*], Pinar Akpinar [d]

[a] Beykent University, İstanbul, Turkey
[b] Mersin University, Mersin, Turkey
[c] Bilecik Şeyh Edebali University, Bilecik, Turkey
[d] Bahçeşehir Cyprus University, Nicosia, N. Cyprus, Turkey

Received 5 September 2022; received in revised form 15 March 2023; accepted 20 March 2023
Available online 28 March 2023

Abstract

Designing lunar shelters with appropriate construction techniques and in-situ materials is a novel and exciting field where many researchers from different countries are working. The first step in working in this field is producing lunar soil simulants on earth that will serve for improving lunar construction materials, as lunar soils are the only in-situ resources available for lunar constructions. Up to date, 9 countries have produced lunar soil simulants and the last contribution has been made by Türkiye as expressed in this study. The technique, of which the properties are explained in this publication, enables the determination of simulant to any lunar soil. When the lunar construction materials are of main concern, the mineral and chemical composition of the lunar soils and the simulants are more critical than their certain geotechnical characteristics since the chemical interactions within the material will primarily define the construction material's performance. Hence, as an important preliminary step in accurate lunar soil simulant production, this study focuses on the determination and matching of the targeted chemical compositions for lunar soil simulants. For this reason, mineralogical analysis of the samples with XRD and chemical compositions with XRF analysis were determined. A novel method was applied during the determination of the simulant, which kept all lunar soil samples with known characteristics as possible targets instead of employing only one targeted soil sample. This enabled the determination of the mentioned new simulant with best fit to a previously known lunar soil sample, while using an attainable budget. The procedure also enabled producing a simulant to a newcomer, the CE-5 Chinese lunar soil, in a very short time.

Keywords: Lunar soils; Regolith; Simulants; Lunar concrete; Jaya algorithm; Apollo missions

1. Introduction

Currently, there are about 900 kg of lunar soil and rock samples on Earth, the most important portion being about 2200 samples brought through Apollo 11, 12, 14, 15, 16, and 17 missions, yielding acquisition of regolith having mass that is close to 382 kg (Crawford, 2012). Remaining samples consists of about 300 g taken from 3 different lunar locations by Luna 16, 20, and 24 missions during Soviet times between 1970 and 1976 (Robinson et al., 2012),

* Corresponding author.
E-mail addresses: cengiztoklu@gmail.com (Y.C. Toklu), nurcan.acikbas@mersin.edu.tr (N. Çalış Açıkbaş), gokhanacikbas@mersin.edu.tr (G. Açıkbaş), erdem.cercevik@bilecik.edu.tr (A.E. Çerçevik), pinar.akpinar@baucyprus.edu.tr (P. Akpinar).

https://doi.org/10.1016/j.asr.2023.03.035
0273-1177/

1.7 kg added very recently by China (Li et al., 2022), and about 500 kg ejected from the Moon toward Earth due to meteorite impacts (Korotev and Irving, 2021).

During an Apollo mission, generally there were more than one sample brought to Earth. The chemical compositions of those samples, and of those which are obtained by averaging the properties of samples taken from the same area, are shown in Table 1, as 18 samples numbered from R01 to R18 where R represents the word "reference" to indicate that these samples are the references for the simulants to be produced to represent them (Zarzycki & Katzer, 2019). Graphical distribution of the chemical components in these samples are shown in Fig. 1. In this figure, and in similar ones in the next paragraphs, the components SiO_2, TiO_2, Al_2O_3, Cr_2O_3, FeO, MnO, MgO, CaO, Na_2O, K_2O, P_2O_5, S, and LOI form the variables in x-axis where LOI is to stand for Loss in Ignition; and the ordinates represent the percentage by weight of the components. Although it is difficult to differentiate 18 curves from each other, Fig. 1 is very illustrative to demonstrate information about lunar soils. One of them is that lunar soil demonstrates important variations from location to location, although there can be a certain uniformity of soils in mare areas and in highlands. This fact can be seen in Fig. 2 for mare areas, in Fig. 3 for highlands, and in Fig. 4 for zones between mares and highlands. It is to be noted that among 18 samples R1-R4, R8, R15-R18 are from mare areas, R9-R14 are from highlands, and R5-R7 are from mixed areas (Zarzycki & Katzer 2019).

These original samples are so precious and so scarce that researchers who would like to work on lunar soil samples for their research, normally cannot have access to use them in their experiments. Thus, they are obliged to produce their own soils which have similar properties to original

Table 1
Comparisons between lunar soils (R Series) and corresponding simulants (S Series).

		Components												
		1	2	3	4	5	6	7	8	9	10	11	12	13
Mission	**NO**	**SiO2**	**TiO2**	**Al2O3**	**Cr2O3**	**FeO**	**MnO**	**MgO**	**CaO**	**Na2O**	**K2O**	**P2 O5**	**S**	**LOI**
Apollo 11	R01	42.100	7.800	13.700	0.300	15.800	0.200	7.900	12.000	0.500	0.100	0.100	0.000	0.000
	S01	42.367	8.987	13.704	0.080	12.353	0.237	7.602	9.217	2.792	0.551	0.168	0.003	1.932
	R02	42.200	7.800	13.600	0.000	15.300	0.200	7.800	11.900	0.470	0.160	0.050	0.000	0.120
	S02	42.383	8.898	13.719	0.080	12.296	0.236	7.573	9.300	2.795	0.552	0.168	0.003	1.990
Apollo 12	R03	46.600	3.600	14.200	0.350	15.400	0.220	9.700	10.400	0.430	0.240	0.000	0.000	0.000
	S03	46.048	5.439	14.394	0.096	10.619	0.210	9.692	8.594	2.940	0.581	0.169	0.002	1.212
	R04	46.000	2.800	12.500	0.410	17.200	0.220	9.700	10.900	0.480	0.240	0.000	0.000	0.000
	S04	45.422	5.464	14.009	0.100	10.568	0.209	10.149	8.881	2.857	0.565	0.165	0.002	1.602
Apollo 14	R05	48.200	1.730	17.600	0.260	10.410	0.140	9.260	11.250	0.610	0.510	0.530	0.000	0.000
	S05	49.585	2.022	16.067	0.082	8.806	0.183	8.636	9.370	3.302	0.651	0.181	0.000	1.107
	R06	47.300	1.600	17.800	0.200	10.500	0.100	9.600	11.400	0.700	0.600	0.000	0.000	0.000
	S06	49.630	1.889	16.012	0.084	8.734	0.181	8.853	9.361	3.290	0.649	0.180	0.000	1.127
	R07	48.100	1.700	17.400	0.000	10.400	0.140	9.400	10.700	0.700	0.550	0.510	0.000	0.000
	S07	49.732	2.042	16.043	0.084	8.850	0.183	8.874	9.124	3.296	0.650	0.180	0.000	0.932
Apollo 15	R08	46.950	1.600	12.700	0.465	16.290	0.217	10.750	10.490	0.330	0.092	0.160	0.070	0.000
	S08	46.546	4.187	14.078	0.109	9.930	0.198	11.219	8.680	2.871	0.569	0.163	0.001	1.442
Apollo 16	R09	45.350	0.490	28.250	0.000	4.550	0.060	5.020	16.210	0.420	0.090	0.100	0.060	0.000
	S09	49.598	1.215	17.258	0.048	8.105	0.172	5.040	11.728	3.563	0.700	0.193	0.000	2.370
	R10	45.200	0.580	26.400	0.160	5.290	0.700	6.100	15.320	0.520	0.140	0.120	0.000	0.000
	S10	50.017	1.225	17.401	0.048	8.174	0.174	5.080	11.354	3.593	0.706	0.194	0.000	2.023
	R11	44.650	0.560	27.000	0.000	5.490	0.700	5.840	15.950	0.440	0.130	0.100	0.000	0.000
	S11	49.801	1.220	17.328	0.048	8.138	0.173	5.059	11.547	3.578	0.703	0.193	0.000	2.202
	R12	44.900	0.470	27.700	0.110	5.010	0.000	5.690	15.700	0.510	0.220	0.160	0.000	0.000
	S12	49.866	1.221	17.350	0.048	8.149	0.173	5.066	11.489	3.582	0.704	0.193	0.000	2.148
	R13	44.770	0.370	28.990	0.000	4.350	0.070	4.200	16.850	0.440	0.060	0.050	0.000	0.000
	S13	49.289	1.207	17.153	0.048	8.055	0.171	5.010	12.004	3.541	0.696	0.192	0.000	2.627
	R14	45.000	0.540	27.300	0.000	5.100	0.300	5.700	15.700	0.460	0.170	0.110	0.000	0.070
	S14	49.814	1.220	17.332	0.048	8.141	0.173	5.061	11.535	3.579	0.703	0.193	0.000	2.191
Apollo 17	R15	41.670	6.520	13.570	0.420	15.370	0.210	10.220	11.180	0.340	0.090	0.060	0.120	0.000
	S15	43.278	7.734	13.304	0.100	11.755	0.227	9.853	8.641	2.704	0.535	0.162	0.003	1.698
	R16	39.820	9.520	11.130	0.460	17.410	0.250	9.510	10.850	0.320	0.070	0.060	0.120	0.000
	S16	39.786	11.163	12.080	0.101	13.522	0.254	9.596	8.403	2.440	0.484	0.155	0.004	2.008
	R17	40.090	9.320	10.700	0.490	17.850	0.240	9.920	10.590	0.360	0.080	0.070	0.130	0.000
	S17	39.677	11.172	11.869	0.106	13.537	0.254	10.111	8.253	2.394	0.475	0.153	0.004	1.989
	R18	42.200	5.090	15.700	0.000	12.400	0.150	10.300	11.500	0.240	0.070	0.000	0.000	0.000
	S18	45.625	5.432	14.275	0.095	10.549	0.209	9.572	9.002	2.915	0.576	0.168	0.002	1.574
CE-5	R19	42.2	5	10.8		22.5	0.28	6.48	11	0.26	0.19	0.23		1.06
	S19	41.97	8.78	13.56	0.08	12.16	0.23	7.58	9.75	2.76	0.55	0.17	0	2.41

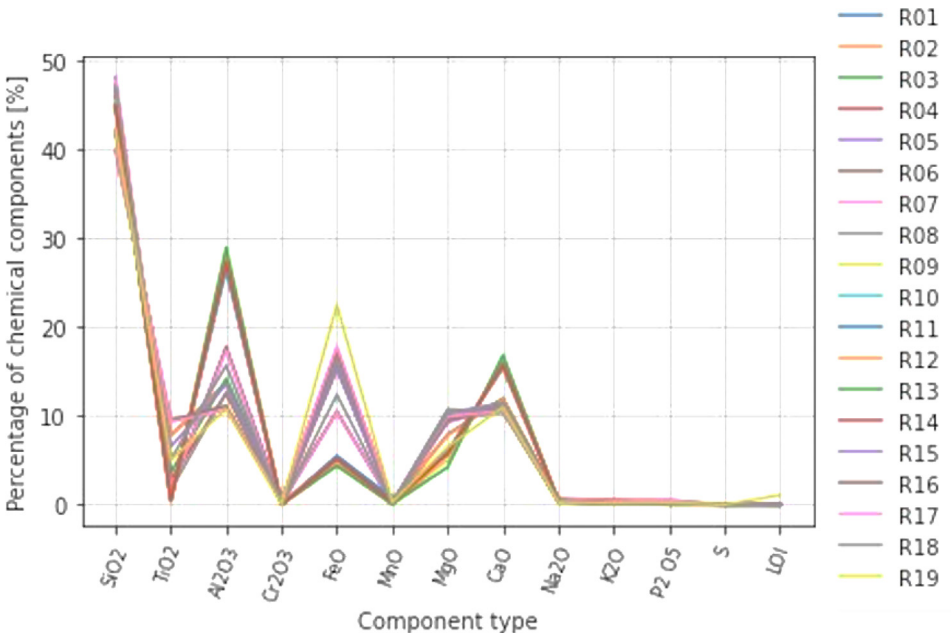

Fig. 1. Graphical representation of percentages of chemical components of all 18 samples related to Apollo missions.

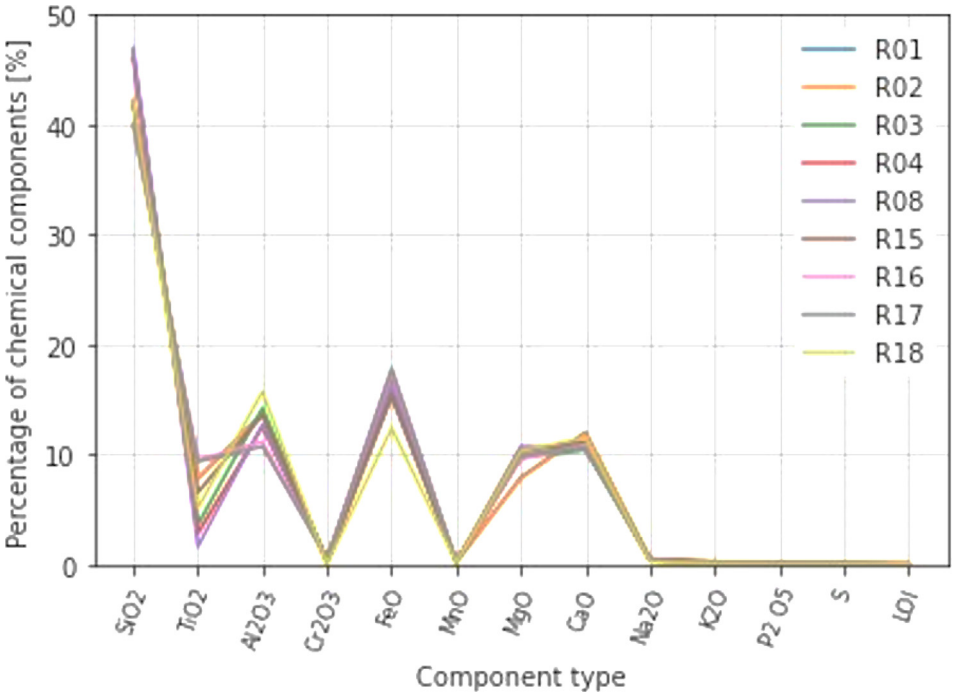

Fig. 2. Graphical representation percentages of chemical components of Apollo samples from mare areas.

ones, i.e., simulants, or obtain simulants from other producers.

Until very recently, organizations and universities in 9 countries were involved in producing simulants; Australia, Canada, China, Germany (with European Union), India, Italy (with European Union), Japan, Korea (South) and Unites States (Toklu and Akpinar 2019(Toklu and Akpinar, 2022). Turkiye became the 10th country in producing lunar soil simulants, without aiming at a certain reference sample, but working on a system that would give products corresponding to any lunar soil.

Production of lunar soil simulants started on different countries in 1970′s, is continuing with an increasing speed (NASA, 2010; Taylor et al., 2016). Until now, tons of such materials are produced and used in different ways. New simulants are produced when old ones are used out, so that some research organizations have produced several versions of their simulants (Taylor & Liu 2010, Taylor et al.,

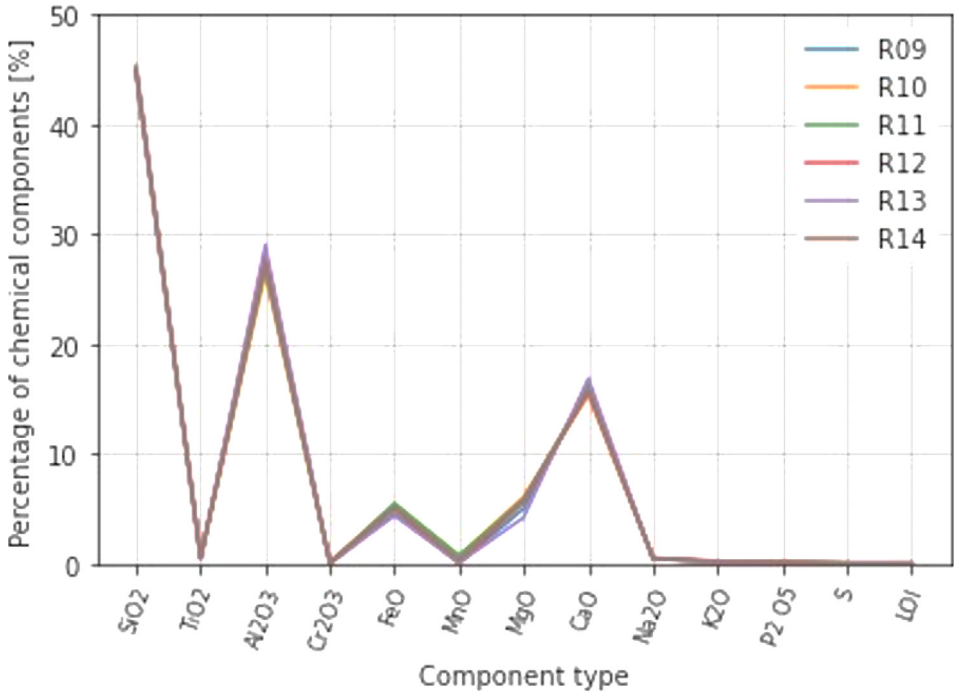

Fig. 3. Graphical representation of percentages of chemical components of Apollo samples from highlands.

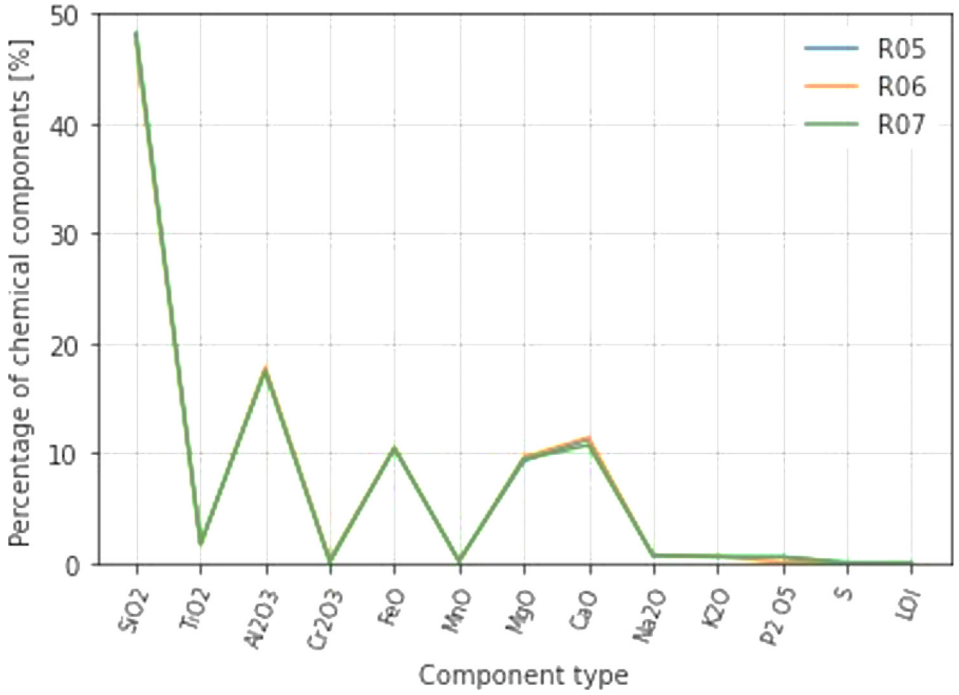

Fig. 4. Graphical representation of percentages of chemical components of Apollo samples from mixed areas.

2016; Toklu and Akpinar 2019. Below are given some examples on resources used in these studies.

- In the series NU-LHT produced in USGS (United States Geological Survey), the required mix was prepared by blending norite, anorthosite, harzburgite and dunite to obtain simulants corresponding to soils in highlands on the Moon (Stoeser et al, 2009).

- In the simulant ALRS-1 produced in Australia, materials of basalt characteristics taken from a mine in New South Wales are used (Bonnano& Bernold, 2015).

- In obtaining Korean simulant KLS Type 1, basalt samples taken from Cheorwon county in this country were the basic materials (Byung-Hyun Ryu et al., 2018).

- In producing DNA-1 and 1A simulant in Italy, materials obtained from Bolsena crater are used (Cesaretti et al., 2014; Marzulli & Cafaro, 2019).

- For producing the Japan simulant FJS-1, materials from many different locations around the world (Japan, USA, Australia, Pakistan, Norway, Mexico, Madagascar) are used and tested (Kanamori et al. 2007).

One of the important areas of use of these lunar simulants within the lunar missions-related science and research is certainly the laboratory studies that aim to produce and test lunar construction materials, which are aimed to be eventually produced on moon using the lunar regolith as the available in situ resource. Voyages to the moon and stationing on moon are the first steps that should be addressed before carrying out other missions in deeper parts of the space. A lunar outpost would definitely need to have constructed facilities such as landing sites and other constructions that will safely facilitate the accommodation of researchers/astronauts, as well as facilitating safe building units for the storage and the utilization of needed lunar experimental investigation equipment. In-situ resource utilization (ISRU) for lunar construction activities seems to be the most feasible approach (Lim et al., 2017; Toklu and Jarvstrat, 2003; Toklu et al., 2013) since the transportation of terrestrial construction materials would be highly costly and technically complicated due to the limitations of lunar voyages (Isachenkov et al.,2021; Oh et al., 2021). Use of a variety of lunar concretes in such lunar construction activities have been proposed by several researchers in the last decades. These varying lunar concrete mixtures are suggested to contain mainly lunar soil as the in-situ resource, either in the function of "cement" in the mix or sometimes in the function of "concrete aggregates", while the binding effect is provided by sulfur-based or polymer-based materials in this latter case. Sulfur-based lunar concretes and polymer-based lunar concretes have been studied in detail and information on their production as well as their performance have been presented in the related-literature (Omar, 1993; Toutanji et al., 2012; Grugel, 2012; Lee et al., 2012; Chen et al., 2018; Su et al., 2019; Oh et al., 2021).

2. Studies in Turkiye for producing lunar soil simulant

This study was initiated to come up with a simulant representing a lunar soil through using samples taken from different locations in Türkiye and some raw materials from mines. Initial studies have shown that, with the application of the adopted procedure, simulants that are representing any lunar soil sample given could be produced, with differing representation ratios of course. For this purpose, relatively undisturbed soil samples were collected from 9 regions known to be volcanic areas in Türkiye. To prepare lunar soil simulants 5 more raw materials were added into volcanic rocks. These are ilmenite and olivine minerals taken from the mines, fly ash and two different types of basalt, one from the Ankara region and the other from the Kayseri region, were added to these samples and the number of samples available was 14. Table 2 gives the sources of the used raw materials to prepare lunar soil simulant.

The chemical composition (elemental and/or oxide contents) of used raw materials, which are shown in Table 3, were determined by Rigaku Primus I model Wavelength Dispersive X-ray Fluorescence (WDXRF) technique. Before XRF and XRD analysis, the samples were ground in a tungsten carbide-coated ring crusher for 30 s at 1000 rpm, and then all samples were sieved under 90 μm. The sieved samples were dried in an oven at 105 °C until they reached constant weight. The fusion method was used for XRF sample preparation. Glass sample discs were obtained with the fusion method by using a 1:10 sample/Lithium Tetraborate mixture. Loss of ignition of the samples were carried out using porcelain crucibles at 1000 °C. In XRF analysis, all elements between Na-U were scanned and the results were given depending on elemental and oxide and by adding ignition losses. Rigaku Miniflex model X-ray powder diffractometer (XRD) was used for mineralogical analysis. XRD analysis were carried out 2θ is between 5 and 70° and the scan speed was 2°/min.

3. Optimization calculations

The percentages given in Table 3 are then compared with the properties of the soils brought through Apollo samples, shown in Table 1. An optimization procedure, like aggregate mix calculations (Toklu 2005, Montemanni et al., 2012) is followed to determine the most appropriate mixes of local soil samples, that would yield compositions as close as possible to the 18 samples, some of which are direct lunar soils, and some are averages obtained by considering several lunar samples collected through same mission.

Table 2
Soil samples collected from various locations in Turkiye.

Code of the sample	Name of the location	Coordinates	
		North	East
A1	Avanos	38°40′20″	34°50′22″
P1	Palandoken	39°50′53.7″	41°16′59.7″
E1	Erciyes Mountain	38°32′33″	35°29′44″
G1	Goreme	38°38′44.4″	34°50′41.9″
K1	Kula	38°34′35″	28°32′55″
S1	Sivrihisar	39°27′11″	31°32′12″
T1	Taurus Mountains	37°45′14″	35°11′16.27″
U1	Uludag	40°05′21.6″	29°08′46.4″
UR	Urgup	38°38′07″	34°53′26″
OL	Olivine	Provided	
UK	Fly ash	Provided	
AB	Ankara Basalt	Provided	
KB	Kayseri Basalt	Provided	
IL	Ilmenite	Provided	

Table 3
Distribution of oxide contents in local soil samples.

SAMPLES	OXIDES % IN WEIGHT												
	SiO_2	TiO_2	Al_2O_3	Cr_2O_3	FeO	MnO	MgO	CaO	Na_2O	K_2O	P_2O_5	S	LOI
A1	47.68	0.91	15.39	0.00	6.57	0.04	2.96	7.28	1.08	4.63	0.14	0.09	12.03
P1	66.22	0.57	16.09	0.01	4.05	0.12	0.62	2.42	5.12	3.94	0.15	0.01	0.70
E1	51.93	0.66	14.86	0.07	7.23	0.24	8.36	10.14	3.85	0.15	0.07	0.00	2.43
G1	7.98	0.03	2.29	0.00	1.01	0.09	17.75	27.88	0.25	0.80	0.05	0.02	41.83
K1	47.34	1.78	18.14	0.00	7.16	0.15	4.61	8.35	5.23	3.49	0.81	0.04	2.89
S1	59.73	0.54	17.97	0.00	4.63	0.12	1.91	6.15	4.64	3.08	0.35	0.01	0.88
T1	1.98	0.00	1.00	0.00	0.33	0.00	0.43	54.21	0.12	0.05	0.03	0.01	41.84
U1	2.26	0.00	1.02	0.00	0.28	0.02	0.39	53.35	0.06	0.14	0.03	0.02	42.41
UR	68.23	0.24	15.45	0.01	2.43	0.09	0.63	3.26	3.13	3.46	0.09	0.02	2.97
AB	59.81	0.98	16.65	0.00	5.00	0.12	2.99	5.94	4.57	1.88	0.34	0.00	1.74
KB	51.77	1.27	18.00	0.05	8.46	0.18	5.25	9.79	3.72	0.73	0.20	0.00	0.57
OL	42.12	0.00	0.85	0.43	8.15	0.15	46.35	0.58	0.00	0.03	0.01	0.00	1.33
UK	59.72	0.86	19.98	0.00	7.68	0.07	2.24	2.39	1.50	2.29	0.16	0.05	3.06
IL	1.83	57.40	0.82	0.07	38.39	0.65	0.58	0.13	0.00	0.00	0.12	0.02	0.00

Let n be the number of chemical components found in each reference sample, and m be the number of soil samples collected from different locations in Turkiye. In the current case n = 13, from SiO_2 to LOI, and m = 14, from A1 to IL, as can be seen in Table 3. The percentages of chemical components found in these soil samples are given by G_{ij}, i = 1, …, n, j = 1, …, m. If $\times = [x_1, x_2, \ldots, x_m]^T$ is the vector representing the proportion of the fractions of soil samples to be used in a blend, the resulting percentages of the chemical components in the final mix would be given by quantities:

$$p_i = \sum_{j=1}^{m} G_{ij}x_j, \; i = 1, 2, \cdots, n \;\; \text{or} \; \mathbf{p} = \mathbf{G} \tag{1}$$

where

$$x_i \geq 0, i = 1, 2, \cdots, m \tag{2a}$$

$$\sum_{i=1}^{m} x_i = 1 \tag{2b}$$

The percentages p_i would be asked to be as close as to the components q_i in the reference sample where i is changing between 1 and n, 13 in this case as indicated above, which means that the vectors **p** and **q** with 13 components will be as close as possible to each other. The distance between the vectors **p** and **q, ||p-q||,** can be measured using different definitions of norms (Toklu 2005). The norm accepted in this study is based on the Euclidean one, with weighting coefficients w_i.

$$\delta = \sqrt{\frac{\sum_{i=1}^{n} w_i (p_i - q_i)^2}{n}} \tag{3}$$

The weighting coefficients are to increase the importance of chemical components with small percentages. They are calculated separately for each reference sample so that the weighing factor and the percentage in the sample are inversely proportional.

The calculations are first carried out 18 times considering all the Apollo samples data given in Table 1, resulting in 18 different mix vectors × each corresponding to a different Apollo sample by minimizing the values δ in Eq. (3). The optimization procedure used in this process is the Jaya algorithm (Rao 2016 Rao et al 2016, Rao 2019, Toklu et al 2021).

Jaya algorithm is a relatively recent one, with an important advantage of having the least number of parameters. Application of this algorithm to the problem in the current case, begins by randomly creating a certain number, n_{pop}, of candidate vectors of which the components satisfy the conditions (2) as stated above. Then using the equations (1) and (3) the discrepancies δ are calculated for each candidate vector. The best vector among them, i.e., the one that yields the smallest δ, is called $\mathbf{g^b}$, and the one that gives the worst result is called $\mathbf{g^w}$. Then the components of all the vectors are revised as indicated in (4), so that the vectors will make a move towards the best one, and away from the worst one.

$$x_i^{t+1} = x_i^t + r_1\left(g_i^b - x_i^t\right) - r_2\left(g_i^w - x_i^t\right) \tag{4}$$

$$x_i^{t+1} = x_i^t + r_1\left(g_i^b - |x_i^t|\right) - r_2\left(g_i^w - |x_i^t|\right) \tag{5}$$

In Eqn (4), t and t + 1 stands for two succeeding cycles, r_1 and r_2 are two random numbers in the range 0 to 1. This step is then followed by a normalization process so that the conditions (2) are satisfied which yields the new candidate vectors completing a cycle. These cycles are then repeated until a predetermined number is satisfied, or convergence criteria becomes satisfied. In Fig. 5, convergence trend of a typical application is shown graphically for three independent runs, where the cycles are shown in the abscissa using a logarithmic scale and corresponding values for δ are shown in y axis.

It is worth mentioning here that in fact the original basic equation for Jaya algorithm is as given in Eqn (5), where the current values of the variables are within an absolute value sign. In this study, the equation (4) is preferred con-

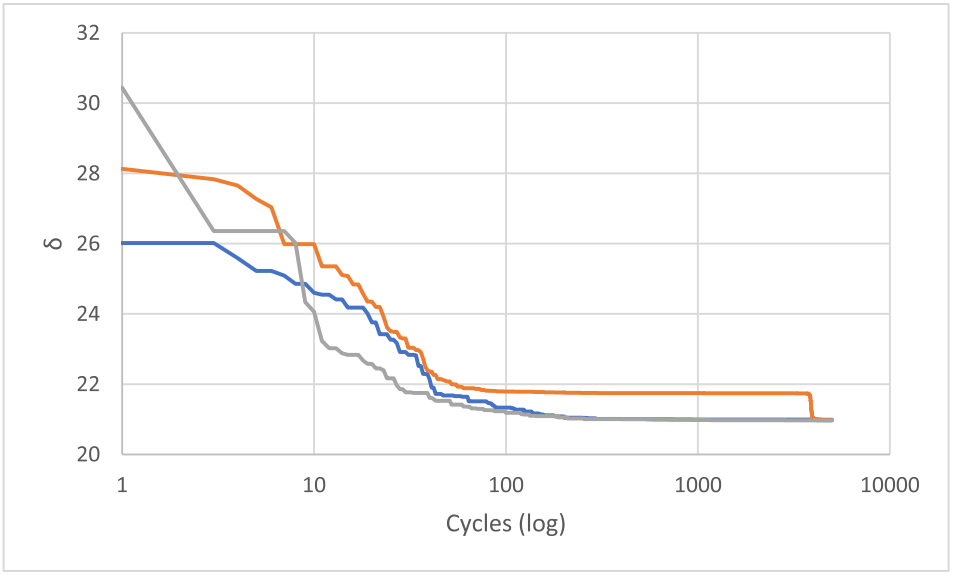

Fig. 5. Convergence trend of the distance δ between the reference soil and the simulant in three independent runs (R19 and S19). The abscissa shows the cycles in logarithmic scale.

sidering that it is theoretically much sounder as compared to the original one. In fact, in the current problem tackled, preference between equations (4) and (5) is immaterial since the variables at hand are all positive.

4. Results and discussion

The obtained XRD graphics of the samples are given in Fig. 6 and the chemical composition of the phases are presented in Table 4. The XRD results showed that A1 sample has Phillipsite, Osumilite, Orthoclase, Albite and Amorphous phases; P1 sample has Albite, Orthoclase, Quartz; E1 has Albite, Quartz, Clinochlore; G1 has Dolomite and Quartz; K1 has Augite, Nepheline, Leucite, Indialite, Muscovite, Pargasite, Amorphous phases; S1 has Albite, Orthoclase, Indialite, Quartz, Edenite; T1 and U1 have similar phases (Calcite and Quartz); UR has Albite, Quartz, Amorphous phases; KB and AB have Plagioclase (Labradorite), Diopside (ferroan), Ferrosilite (magnesian); UK has Quartz, Mullite, Magnetite, Amorphous phase; IL

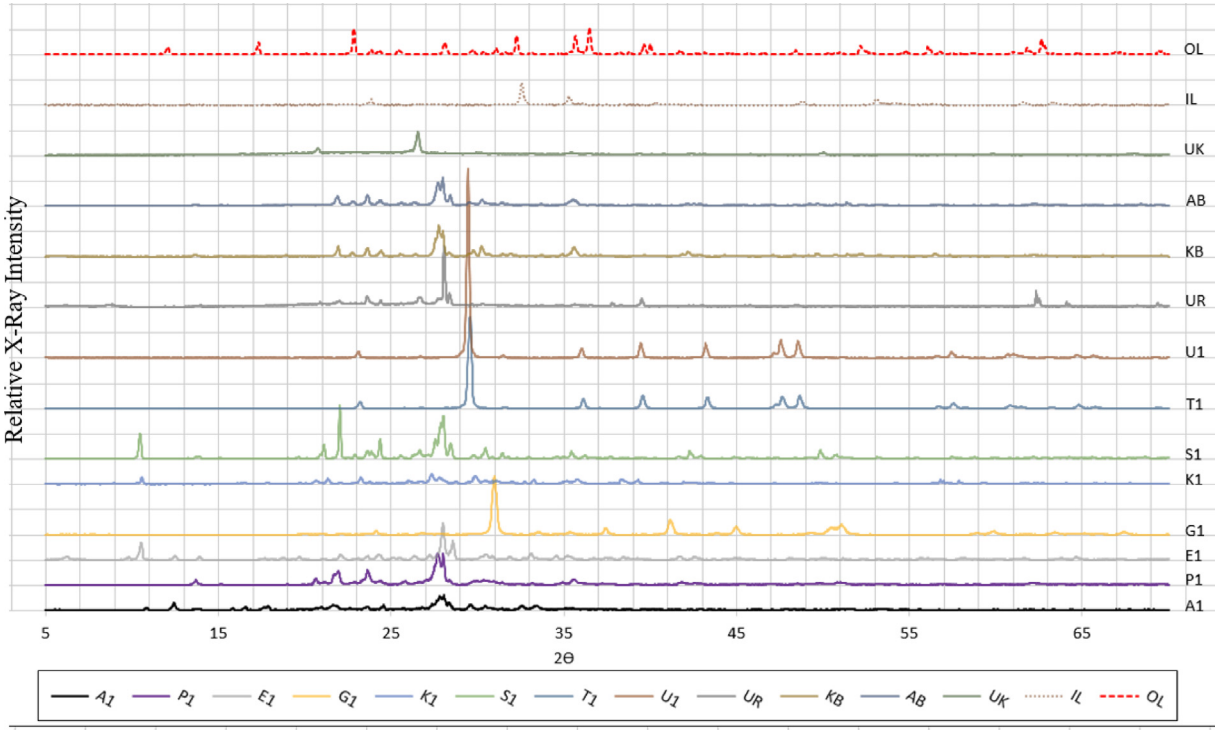

Fig. 6. XRD graph of local samples.

Table 4
Mineralogical analysis of samples.

Phases in samples	
Samples	**Phases**
A1	Phillipsite, Osumilite, Orthoclase, Albite, Amorphous phase
P1	Albite, Orthoclase, Quartz
E1	Albite, Quartz, Clinochlore
G1	Dolomite, Quartz
K1	Augite, Nepheline, Leucite, Indialite, Muscovite, Pargasite, Amorphous phase
S1	Albite, Orthoclase, Indialite, Quartz, Edenite
T1	Calcite, Quartz
U1	Calcite, Quartz
UR	Albite, Quartz, Amorphous phase
KB	Plagioclase (Labradorite), Diopside (ferroan), Ferrosilite (magnesian)
AB	Plagioclase (Labradorite), Ferrosilite (magnesian), Diopside (ferroan)
UK	Quartz, Mullite, Magnetite, Amorphous phase
IL	Ilmenite, Rutile, Quartz
OL	Forsterite (ferroan), Enstatite (ferroan), Lizardite

Chemical formula of phases		
Phases	**JCPDS Card Number**	**Chemical Formula**
Phillipsite	(01–076-2793)	(Ca0.5, K, Na, Ba0.5)4–7(Al4-7Si12-9O32).12H2O
Osumilite	(01–084-1723)	(K,Na)(Fe2+,Mg)2(Al,Fe3+)3(Si,Al)12O30
Albite	(01–071-1540)	NaAlSi3O8
Orthoclase	(01–071-1540)	KAlSi3O8
Quartz	(01–075-8320)	SiO2
Clinochlore	(01–075-8790)	(Mg, Fe2)5, Al(Si3Al)O10(OH)8
Dolomite	(01–074-7803)	Ca.Mg.2(CO3)
Augite	(00–041-1483)	(Ca,Na)(Mg,Fe,Al,Ti)(Si,Al)2O6
Nepheline	(01–083-2279)	Na3KAl4Si4O16
Leucite	(01–076-8736)	KAlSi2O6
Indialite	(01–089-1486)	Mg2Al4Si5O18
Muscovite	(01–076-0637)	KAl2(AlSi3O10)(F,OH)2
Pargasite	(01–089-7541)	NaCa2(Mg4Al)(Si6Al2)O22(OH)2
Edenite	(01–084-2123)	$NaCa_2Mg_5(Si7Al)O22OH2$
Mullite	(00–001-0613)	3Al2O3.2SiO2
Magnetite	(01–086-1354)	Fe3O4
Plagioclase(Labradorite)	(01–083-1368)	$Ca_{0.65}\ Na_{0.32}\ (Al_{1.62}\ Si_{2.38}\ O_8)$
Diopside (Ferroan)	(01–073-9803)	$(Mg_{0.88}\ Fe_{0.09}\ Al_{0.03})\ (Ca_{0.95}\ Na_{0.01}\ Fe_{0.04})\ (Si_{1.98}\ Al_{0.02}\ O_6)$
Ferrosilite (Magnesian)	(01–088-1919)	$(Mg\ Fe)_2Si_2O_6$
Ilmenite	(00–003-0778)	$Fe^{+2}TiO_3$
Rutile	(01–086-1630)	TiO2
Forsterite (Ferroan)	(01–072-2460)	$Mg_{1.85}\ Fe_{0.15}Si\ O_4$
Enstatite (Ferroan)	(01–083-0669)	$(Fe_{0.115}\ Mg_{0.885})\ (Fe_{0.383}\ Mg_{0.617})\ Si_2O_6$
Lizardite	(01–082-1837)	$Mg_3(Si_2O_5)(OH)_4$

has Ilmenite, Rutile, Quartz; OL has Forsterite (ferroan), Enstatite (ferroan), Lizardite phases.

According to XRF analysis loss of ignition values are changing between 0 (for IL sample) and 42.41 (for U1 sample). The oxide amounts in the samples vary in the following ranges: SiO2 is 1.83 to 68.23; TiO2 is 0 to 57.4; Al2O3 is 0.82 and 19.98; Cr2O3 is 0 and 0.43; FeO is 0.28 and 38.39; MnO is 0 and 0.65; MgO is 0.39 and 46.35; CaO is 0.13 and 54.21; Na2O is 0 and 5.23; K2O is 0 and 4.63; P2O5 is 0.01 and 0.81; S is 0 and 0.09.

Table 1 summarizes the results obtained after the application of the method described showing the percentages of the chemical components between reference soils (R) and the simulants (S). Indeed, in this table, the upper line, from R01 to R18, shows the components of lunar soils, q_i, the lower ones, from S01 to S18, show the corresponding percentages of the simulants in question, p_i. Table 5 shows the distances δ for all the 18 Apollo soils. It is seen from this table that although mixes are obtained for all Apollo soils, the best fit is 7th soil with δ as 10.00, from Apollo 14; and the worst fit is for the 13th soil, with δ as 27.14 from Apollo 16. Figs. 7 and 8 illustrate the best fit, between R07 and S07 and the worst fit, between R13 and S13. Fig. 9 shows a photo of a sample of the new simulant named as TBG-1, with the best fit to Apollo soil R07. It is to be noted that although 14 samples from Turkiye are considered in determining mixes to yield simulants, the first 9 of them, i.e., those taken from volcanic areas (See Table 2), have negligibly small percentages in the mixes, as the optimization calculations revealed.

It has been seen that the range of percentages of chemical components in a lunar soil is quite high and may vary

Table 5
Discrepancies δ calculated between the simulants obtained and the Apollo samples.

TARGET	R01	R02	R03	R04	R05	R06	**R07**	R08	R09
DISTANCE δ	13.43	12.62	14.93	19.16	10.82	11.14	**10.00**	18.81	25.90
TARGET	R10	R11	R12	**R13**	R14	R15	R16	R17	R18
DISTANCE δ	22.79	23.64	24.40	**27.14**	23.97	13.36	13.72	14.28	12.02

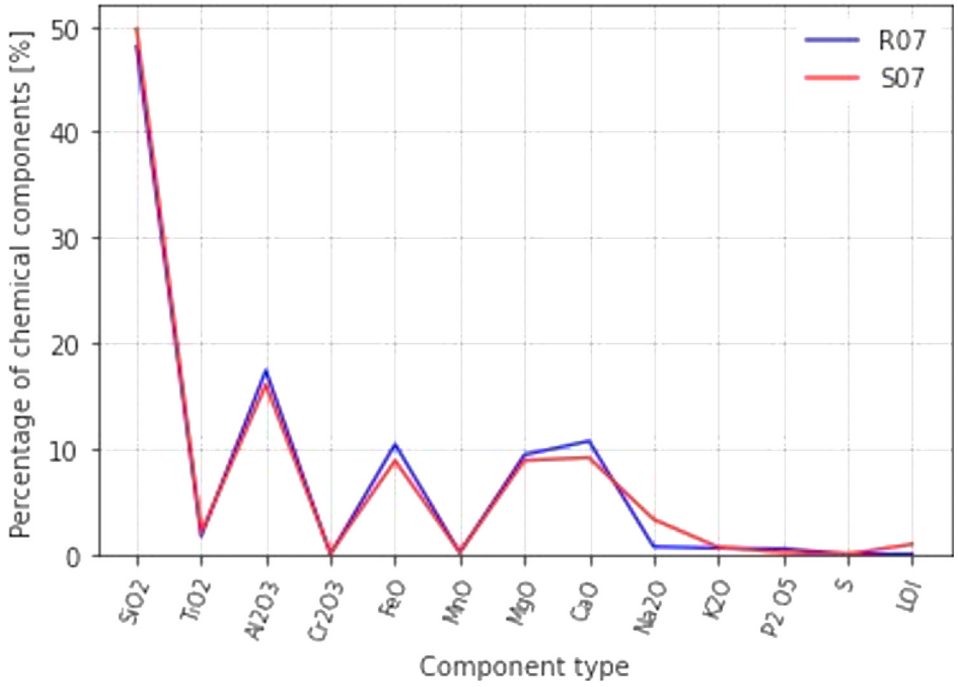

Fig. 7. The best fit. Comparison of percentages of the chemical components of Apollo 14 soil R07 and the corresponding simulant S07, named TBG-1. $\delta = 10.00$.

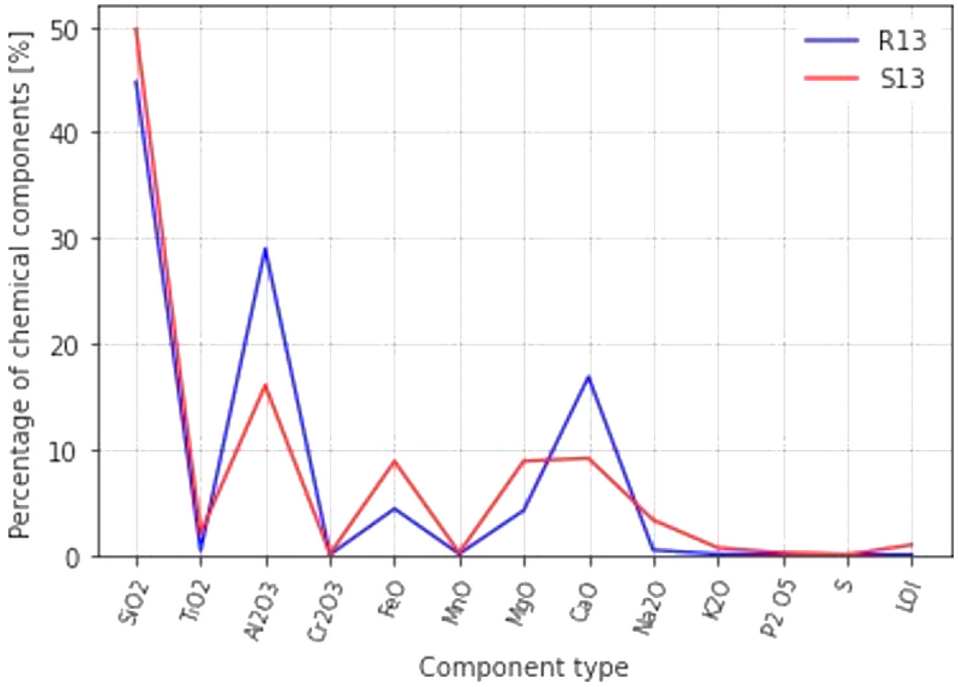

Fig. 8. The worst fit. Comparison of percentages of the chemical components of Apollo soil R13 and the corresponding simulant S13. $\delta = 27.14$.

Fig. 9. The best simulant obtained, TBG-1.

between 0% and almost 60% (See Fig. 1 for instance). This range necessitates the use of weighing factors in making comparisons between candidates since otherwise components with small percentages should not have any importance in the determination of the mixes. To overcome this problem, a convenient method would be to assign weighing factors 100 and 1 to the smallest and highest percentages, respectively, and to assign weighing factors calculated accordingly for the intermediate ones. It is obvious that choice of other types of weighing factors will change the final mix. Fig. 7 comparing the percentages of components between the reference soil R07 and the corresponding simulant S07 indicates that the choice of weighing factors explained above can be considered as a valid one.

Certainly, the weighing factors used in the calculations have an effect in the final product. Although it is evident that other choices than the one used in this study will result in simulants different than the ones found in this study, it is considered that the differences will not be of great importance. The same consideration is valid also for the measurements of the differences between original soils and their simulants. Other choices of norms other than Euclidean will certainly result in different solutions, but again, the differences will not be of a degree invalidating the choices made in this study.

The latest soil sample brought to Earth is the one taken from the Moon through Chinese mission CE-5. The properties of that soil are shown as R19 in Table 1 as given in a recent publication (Li et al. 2022). As the procedure described in this study permits making calculations for any type of soil, it was possible to determine a mix S19 with smallest discrepancy to the reference soil. The chemical composition of the simulant S19 is shown in Table 1 as calculated following the procedure described in this study. The distance δ between R19 and S19 is 20.96 as calculated using Eqn. (3), with the percentages compared as in Fig. 10.

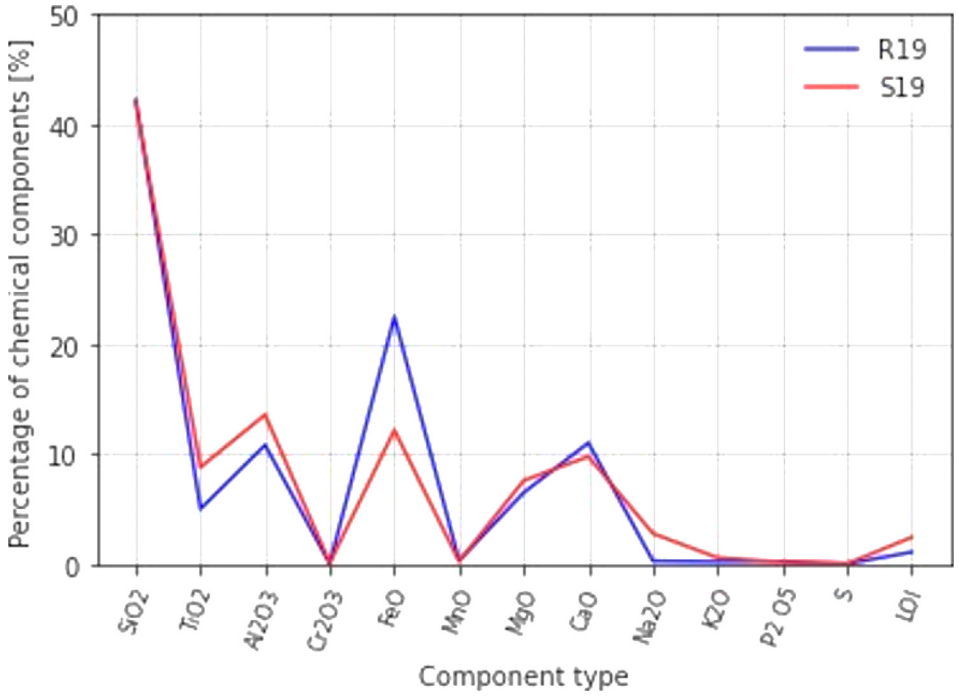

Fig. 10. Comparison of percentages of the chemical components of soil R19 brought through Chinese mission CE-5 and the corresponding simulant S19. $\delta = 20.96$.

5. Conclusions

In this study, a procedure is followed not to just find a simulant corresponding to a predetermined soil sample, but to find mixes with properties as close as possible to all soil samples with known chemical properties. This approach will enable the researchers to have several simulants at hand with the same samples taken from sources on Earth. The conditions that are necessary to be able to apply this procedure is to have as much as terrestrial soil samples at hand and an optimization algorithm which will be helpful in determining the best mixes. The algorithm used in this study is Jaya algorithm to which a correction note is added.

This procedure enabled first the determination of simulants to 18 lunar soils based on those brought through Apollo missions making use of 14 terrestrial soil samples taken from volcanic areas or from local quarries and mines. The comparisons made have shown that the discrepancies between the reference soils and the simulants are not the same and the best fit is obtained for an Apollo 14 soil. The corresponding simulant is called TBG-01.

The procedure explained has also been applied on a soil brought from the Moon only a year ago by the Chinese mission CE-5 and with chemical properties published very recently. The versatility of the procedure explained enabled determination of the simulant corresponding to this soil in a very short time with no extra effort proving that simulants can be obtained for every extraterrestrial soil sample rapidly and with sufficient accuracy.

It is obvious that being able to produce different simulants from a given set of terrestrial samples will also be helpful in making further research with these simulants, for instance in trying to produce the best space concrete. Having more simulants at hand will enable the researchers to make comparisons between space concretes produced using soils belonging to different locations on space bodies.

Another conclusion that can be derived from this study is the affordable cost of this research. This conclusion may encourage more studies on lunar soil research to be made at institutions that are without major financial strength, thus globalization of space research in the direction of producing lunar construction materials would be facilitated.

Declaration of Competing Interest

The authors declare that they have no known competing financial interests or personal relationships that could have appeared to influence the work reported in this paper.

Acknowledgements

This work has been supported by Beykent University Scientific Research Projects Coordination Unit. Project Number: 2018-19-BAP-01, 2021.

References

Bonnano, A., Bernold, L.E., 2015. Exploratory review of sintered lunar soil based on the results of the thermal analysis of a lunar soil simulant. J. Aerosp. Eng. 28, 04014114.

Cesaretti, G., Dini, E., De Kestelier, X., Colla, V., Pambaguian, L., 2014. Building components for an outpost on the Lunar soil by means of a novel 3D printing technology. Acta Astronaut. 93, 430–450. https://doi.org/10.1016/j.actaastro.2013.07.034.

Chen, T., Chow, B.J., Zhong, Y., Wang, M., Kou, R., Qiao, Y., 2018. Formation of polymer micro-agglomerations in ultralow-binder-content composite based on lunar soil simulant. Adv. Space Res. 61 (3), 830–836. https://doi.org/10.1016/j.asr.2017.10.050.

Crawford, I., 2012. The scientific legacy of Apollo. Astron. Geophys. 53 (6), 6–24.

Grugel, R.N., 2012. Integrity of sulfur concrete subjected to simulated lunar temperature cycles. Adv. Space Res. 50 (9), 1294–1299. https://doi.org/10.1016/j.asr.2012.06.027.

Isachenkov, M., Chugunov, S., Akhatov, I., Shishkovsky, I., 2021. Regolith-based additive manufacturing for sustainable development of lunar infrastructure – an overview. Acta Astronaut. 180 (September 2020), 650–678. https://doi.org/10.1016/j.actaastro.2021.01.005.

Kanamori, H., Matsui, K., Miyahara, A., & Aoki, S. (2007). Development of new lunar soil simulants in Japan. In *Space Resources Roundtable VIII: Program and Abstracts (LPI Contribution No. 1332)* (Vol. 1332, pp. 35-36).

Korotev, R.L., Irving, A.J., 2021. Lunar meteorites from northern Africa. Meteorit. Planet. Sci. 56 (2), 206–240.

Lee, J., Chang, B. C., Lee, S., & Lee, T. S. (2012). Feasibility study on lunar concrete landing pad. Earth and Space 2012 - Proceedings of the 13th ASCE Aerospace Division Conference and the 5th NASA/ASCE Workshop on Granular Materials in Space Exploration, April, 128–134. https://doi.org/10.1061/9780784412190.015.

Li, C., Hu, H., Yang, M. F., Pei, Z. Y., Zhou, Q., Ren, X., ... & Ouyang, Z. (2022). Characteristics of the lunar samples returned by the Chang'E-5 mission. *National Science Review*, *9*(2), nwab188

Lim, S., Prabhu, V.L., Anand, M., Taylor, L.A., 2017. Extra-terrestrial construction processes – advancements, opportunities and challenges. Adv. Space Res. 60 (7), 1413–1429. https://doi.org/10.1016/j.asr.2017.06.038.

Marzulli, V., Cafaro, F., 2019. Geotechnical properties of uncompacted DNA-1. a lunar simulant. J. Aerosp. Eng. 32 (2), 04018153.

Montemanni, R., Toklu, N. E., Toklu, Ş. Ç., And Toklu, Y. C. (2012) "Aggregate Blending via Robust Linear Programming", Journal of Construction Engineering and Management. 138(2): 188-196. [SCIE] doi:10.1061/(ASCE)CO.1943-7862.0000422

NASA- Simulant Working Group of the Lunar Exploration Analysis Group and Curation and Analysis Planning Team for Extraterrestrial Materials. (2010). *Status of lunar regolith simulants and demand for Apollo lunar samples*.

Oh, K., Yi, H., Chen, T., Chow, B.J., Kou, R., Qiao, Y., 2021. Impact formation of ultralow-binder-content composite "lunar cement". CEAS Space J. 13 (2), 183–187. https://doi.org/10.1007/s12567-020-00327-3.

Omar, H. A. (1993). Production Using of Lunar Concrete. Final Research Report for JoVe NASA Grant NAG8 -278. https://ntrs.nasa.gov/api/citations/19980001900/downloads/19980001900.pdf

Rao, S.S., 2019. Engineering optimization: theory and practice. John Wiley & Sons.

Rao, R.V., More, K., Taler, J., Ocłoń, P., 2016. Dimensional optimization of a micro-channel heat sink using Jaya algorithm. Appl. Therm. Eng. 103, 572–582.

Rao, R. (2016). Jaya: A simple and new optimization algorithm for solving constrained and unconstrained optimization problems. *International Journal of Industrial Engineering Computations*, *7*(1), 19-34

Robinson, M.S., Plescia, J.B., Jolliff, B.L., Lawrence, S.J., 2012. Soviet lunar sample return missions: landing site identification and geologic context. Planet. Space Sci. 69 (1), 76–88.

Ryu, B.H., Wang, C.C., Chang, I., 2018. Development and geotechnical engineering properties of KLS-1 lunar simulant. J. Aerosp. Eng. 31 (1), 04017083.

Stoeser, D. B., Rickman, D. L., & Wilson, S. (2010). Preliminary Geological Findings on the BP-1 Simulant. Nasa Tm, 2010–216444, 24. http://hdl.handle.net/2060/20100036344

Su H., Hong Y., Chen T., Kou R., Wang M., Zhong Y., Q. Y. (2019). Fatigue Behavior of Inorganicorganic Hybrid "Lunar Cement". Nature Scientific Reports, 9, 2238. https://doi.org/https://doi.org/10.1038/s41598-019-38799-x.

Taylor, L. A., & Liu, Y. (2010). Important considerations for lunar soil simulants. In *Earth and Space 2010: Engineering, Science, Construction, and Operations in Challenging Environments* (pp. 106-118).

Taylor, L.A., Pieters, C.M., Britt, D., 2016. Evaluations of lunar regolith simulants. Planet. Space Sci. 126, 1–7. https://doi.org/10.1016/j.pss.2016.04.005.

Toklu, Y.C., 2005. Aggregate blending using genetic algorithms. Comput. Aided Civ. Inf. Eng. 20 (6), 450–460.

Toklu, Y.C., Akpinar, P., 2022. Lunar soils, simulants and lunar construction materials: an overview. Adv. Space Res. 70 (3), 762–779.

Toklu, Y. C., Akpınar, P., (2019) "Lunar soil simulants- An assessment", in: Proc. 9th Int. Conf. Recent Adv.Sp.Technol. RAST 2019. https://doi.org/10.1109/RAST.2019.8767790.

Toklu Y.C., Jarvstrat, N. (2003). Design and Construction of a Self-Sustainable Lunar Colony with In-Situ Resource Utilisation. In J. Cha; R. Jardim Goncalves; A. Steiger Garcao Swets&Zeitlinger, Lisse (Ed.), Proceedings of the 10th ISPE International Conference On Concurrent Engineering: Research and Applications. (CE: The Vision for Future Generation in Research and Applications) ISBN 90 5809 622 X (pp. 623–628).

Toklu, Y.C., Bekdaş, G., Niğdeli, S.M., 2021. Metaheuristics for Structural Design and Analysis. John Wiley & Sons.

Toklu, Y. C., Temür, R., Bekdaş, G., & Uzun, F. (2013, June). Space applications of tensegric structures. In *2013 6th International Conference on Recent Advances in Space Technologies (RAST 2013)* (pp. 29-32). IEEE.

Toutanji, H.A., Evans, S., Grugel, R., 2012. Performance of lunar sulfur concrete in lunar environments. Constr. Build. Mater. Build. Mat. 29, 444–448. https://doi.org/10.1016/j.conbuildmat.2011.10.041.

Zarzycki, P.K., Katzer, J., 2019. Multivariate comparison of lunar soil simulants. J. Aerosp. Eng. 32 (5), 06019005.